JOURNAL OF MATERIALS SCIENCE **30** (1995) 1613–1616

Analytical electron microscopy study of a new phase in an equiatomic $Ti_{50}Pd_{50}$ Alloy

L. CHANG
Materials Research Laboratories, Industrial Technology Research Institute, Chutung, Hsinchu 310, Taiwan

Y. C. LO, S. K. WU
Institute of Materials Science and Engineering, National Taiwan University, Taipei, 106, Taiwan

Analytical electron microscopy has been used to study a new phase found in a Ti_{50} Pd_{50} alloy. The new phase was formed as ellipsoidal particles along the grain boundaries of the martensitic matrix. The crystal structure was identified as trigonal, with lattice parameters of $a = 0.83$ nm, and $c = 2.62$ nm, and point group $\bar{3}m$. The phase contains 68–73 at% Ti (48–54 wt% Ti).

1. Introduction

The thermoelastic martensitic transformation causing the shape-memory effect at around room temperature in nearly equiatomic TiNi shape-memory alloys has long been studied [1–3]. Another equiatomic alloy, $Ti_{50}Pd_{50}$, had been reported to exhibit a shape-memory effect at high temperature (about 540°C) and undergo a high-temperature martensitic transformation [4–8]. From a high-temperature X-ray diffraction study [9], the equiatomic $Ti_{50}Pd_{50}$ alloy was found to undergo a martensitic transformation from cubic B2 (CsCl type) phase to the orthorhombic B19 (AuCd type) phase. The M_s and A_s temperatures were 540 and 555°C, respectively. From the Ti–Pd phase diagram [10], it is seen that the equilibrium phases coexisting with $Ti_{50}Pd_{50}$ phase are Ti_2Pd and Ti_2Pd_3. In the present paper, a new titanium-rich phase coexisting with $Ti_{50}Pd_{50}$ phase is described which has been observed in the $Ti_{50}Pd_{50}$ alloy during a TEM study of the B2 → B19 martensitic transformation. The crystal structure and the chemical composition of this new phase were determined in the present work by using analytical electron microscopy.

2. Experimental procedure

A $Ti_{50}Pd_{50}$ alloy was prepared from 99.7 % pure titanium and 99.9 % pure palladium using a conventional non-consumable tungsten electrode vacuum arc melter under a controlled protective argon atmosphere. The as-melted button was homogenized at 1050°C for 72 h in a vacuum furnace, and then hot-rolled to about 1 mm thickness. The bulk chemical composition was measured by quantitative analysis of X-ray energy dispersive spectroscopy (EDS) using pure titanium and palladium metals as standard. The *ZAF*(*Z*, the atomic number factor; *A*, the absorption factor; *F*, the characteristic fluorescence correction) correction method was employed to obtain the composition. The results showed that the alloy consists of 70.0 wt % Pd and 30.0 wt % Ti (~ 51.2 at % Pd and 48.8 at % Ti). Specimens for TEM observation were carefully cut from the hot-rolled plates. These specimens (3 mm diameter discs) were then solution treated at 1000° C for 1 h in evacuated quartz tubes and then quenched into water at room temperature. TEM specimens were prepared by twin-jet electropolishing with an electrolyte consisting of 20% H_2SO_4 and 80% CH_3OH by volume. Analytical electron microscopy was done on a Jeol JEM 2000FX scanning transmission electron microscope (STEM) equipped with Link LZ5 EDS detector and Gatan 667 parallel electron energy loss spectrometer (EELS). The operating voltage was 200 kV. In the present study, the elemental analysis of the new phase particle was performed on thin films and EDS for quantitative chemical microanalysis was performed using the Link RTS2/FLS thin-foil program. Careful examination was taken to ensure that the probed areas were less than 100 nm thick and there were no strong two-beam reflections. Each spectrum was acquired to have over 10 000 counts for titanium and palladium peaks to reduce the statistical errors.

3. Results and discussion

3.1. Identification of crystal structure

Fig. 1 shows a typical electron micrograph in which the heavily twinned spear-like martensite is clearly seen. In addition, a few particles along grain boundaries can be observed. The higher magnified micrograph of the particles is shown in Fig. 2, revealing that the morphology of the particles is near ellipsoidal. The particle size is in the submicrometre range. Image analysis shows that the volume percentage of the particles is about 2 %. The convergent beam electron

0022-2461

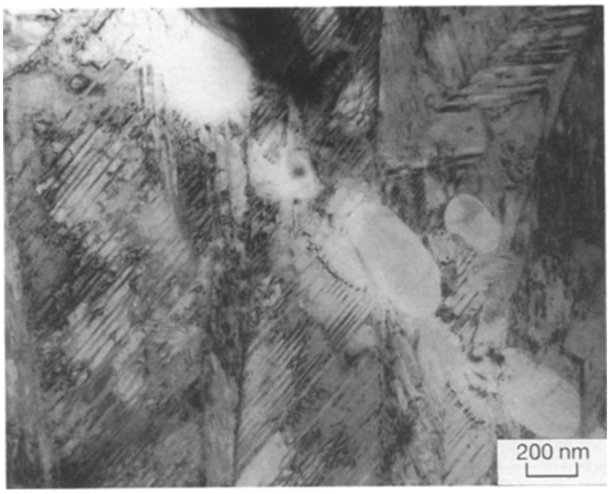

Figure 1 Bright-field image of the $Ti_{50}Pd_{50}$ alloy showing the second-phase particles.

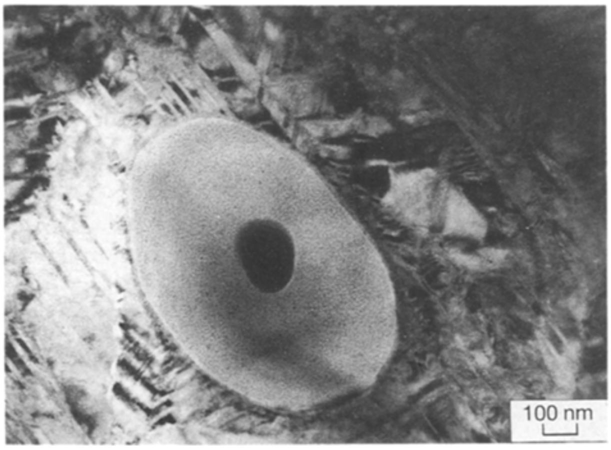

Figure 2 Bright-field image of the second-phase particle showing its morphology is near ellipsoidal. The dark spot in the centre of the particle was caused by the contamination during EDS acquisition and CBED examination.

diffraction (CBED) patterns from such particles are shown in Fig. 3. The zero-order Laue zone (ZOLZ) pattern in Fig. 3a exhibits $6mm$ symmetry, but the whole pattern in Fig. 3b demonstrates that the symmetry is $3m$. According to Loretto [11] and Buxton *et al.* [12], the deduced diffraction group for these particles is $6_R mm_R$, leading to the point group to be either $\bar{3}m$ or $m3m$. Because this is the highest symmetry pattern found in all orientations, and no $4mm$ symmetry was observed, we can conclude that the point group is $\bar{3}m$. Further evidence from other CBED patterns is shown in Fig. 4, in which the whole pattern has only m symmetry (see Fig. 4b), although the ZOLZ pattern has $2mm$ (see Fig. 4a). The diffraction group is then $2_R mm_R$, giving the point group of $\bar{3}m$ as well. Thus the point group of the particle is certainly to be $\bar{3}m$, belonging to trigonal crystal system. Based on the CBED and selected-area diffraction (SAD) patterns in various zones, the lattice parameters of the rhombohedral structure were determined to be $a = 0.83 \pm 0.01$ nm and $c = 2.62 \pm 0.05$ nm in hexagonal axis notation. The observed interplanar spacings are listed in Table I. The possible space groups which have $\bar{3}m$ point group symmetry are $P\bar{3}1m$ (162), $P\bar{3}1c$ (163), $P\bar{3}m1$ (164), $P\bar{3}c1$ (165), $R\bar{3}m$ (166), $R\bar{3}c1$ (167) [13]. Numbers in parentheses refer to the number of the space group in the "International Tables for Crystallography" [13]. Except $P\bar{3}1m$ and $P\bar{3}m1$ space groups, all others have reflection conditions of $l = 2n$ or $l = 3n$ for $(hkil)$ planes. As the $(1\bar{1}01)$ reflection were observed with no dynamic absence on the diffraction discs, there may be no extra reflection conditions for the phase. Hence, the possible space group can be either $P\bar{3}1m$ or

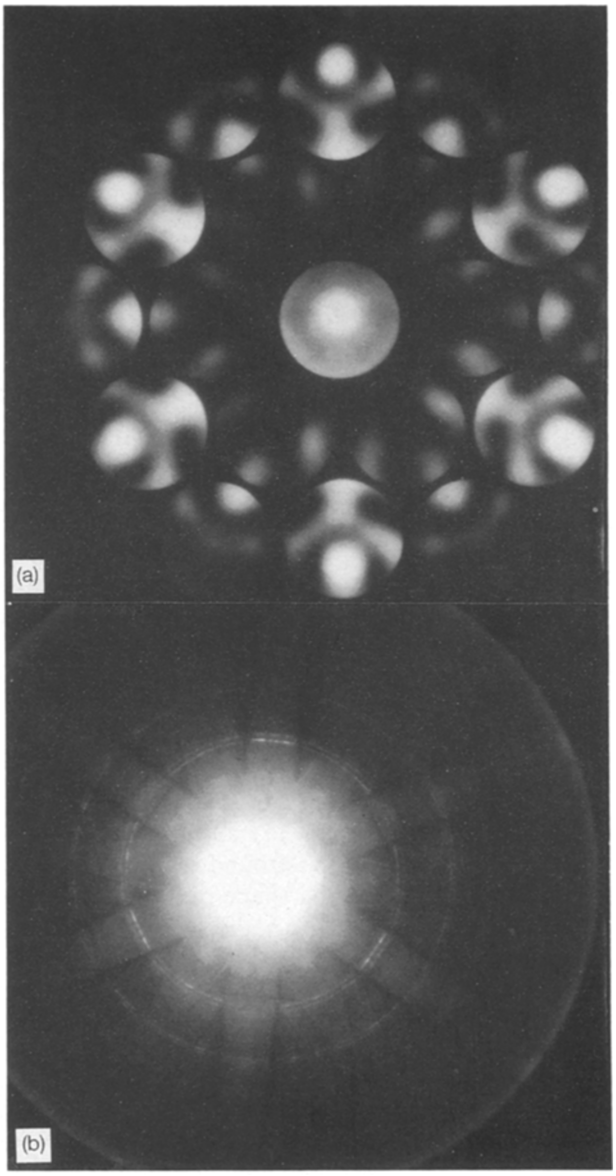

Figure 3 Convergent-beam electron diffraction pattern showing symmetry information: (a) zero-order Laue zone, (b) whole pattern.

TABLE I Observed interplanar spacings from the trigonal phase in $Ti_{50}Pd_{50}$ alloy

Plane	*d*-spacing (nm)
0003	0.87
$1\bar{1}00$	0.72
$1\bar{1}01$	0.69
$1\bar{1}02$	0.63
$1\bar{1}03$	0.55
$2\bar{1}\bar{1}0$	0.42

$P\bar{3}m1$. No distinction between them can be made from the available experimental evidence.

3.2. Determination of chemical composition

No light elements such as carbon and oxygen could be detected in any of the EDS and EELS spectra. The typical EDS spectra from a particle and the matrix are shown in Fig. 5a and b, respectively. It is apparent that the particles are enriched with titanium. Because no stoichiometric compounds containing titanium and palladium elements were available to be used as TEM thin-foil standard, we assume that the matrix has the same compositions as the bulk, based on the fact that the volume fraction of the second-phase particles is very small in comparison with the matrix. The average intensity ratio of Pd/Ti in the matrix obtained from ten EDS spectra is 1.11. This results in a k_{PdTi} factor 2.1 ± 0.2 (in three standard deviations) in a Cliff–Lorimer thin film criterion [14]. The intensity ratio of Pd/Ti obtained from 11 particles varies from 0.41–0.51. Therefore, the particles contain about 68–73 at %Ti (48–54 wt % Ti). The only possible phase which can exist with such compositions is β–Ti (see the Ti–Pd phase diagram in [9]). However, β–Ti has body-centred cubic structure (space group:Im 3m). No such phase of 68–73 at % Ti with trigonal structure has been reported in the published literature.

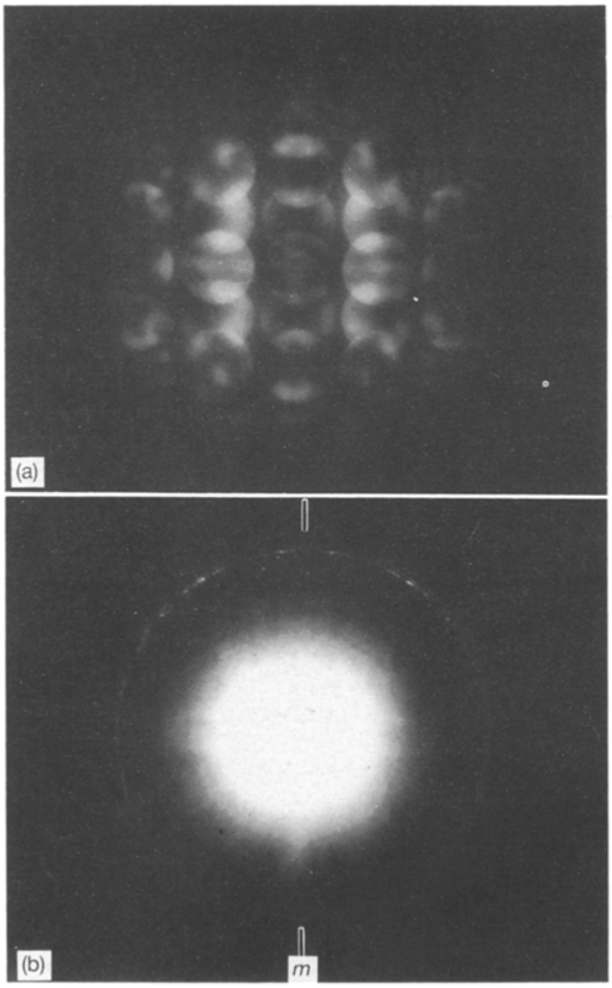

Figure 4 Convergent-beam electron diffraction pattern showing the symmetry information: (a) zero-order Laue zone, (b) whole pattern.

3.3. Discussion of the new phase

The lattice image of a particle obtained along the $[1\bar{1}01]$ zone axis is shown in Fig. 6. The interphase boundaries are relatively smooth on a nanometre scale. No orientation relationship between particles and the matrix can be found. Although it is not clear how the new phase is formed, some clues can still be drawn from microstructure observations. The presence of the second phase at grain boundaries of the martensitic matrix may indicate that the precipitation has already occurred before martensitic transformation. Also, few defects have been observed in the particles, indicating that it has a long thermal history. It is highly possible that during solidification the alloy undergoes the decomposition into the second phase and the matrix phase. Very recently, Yi *et al.* have

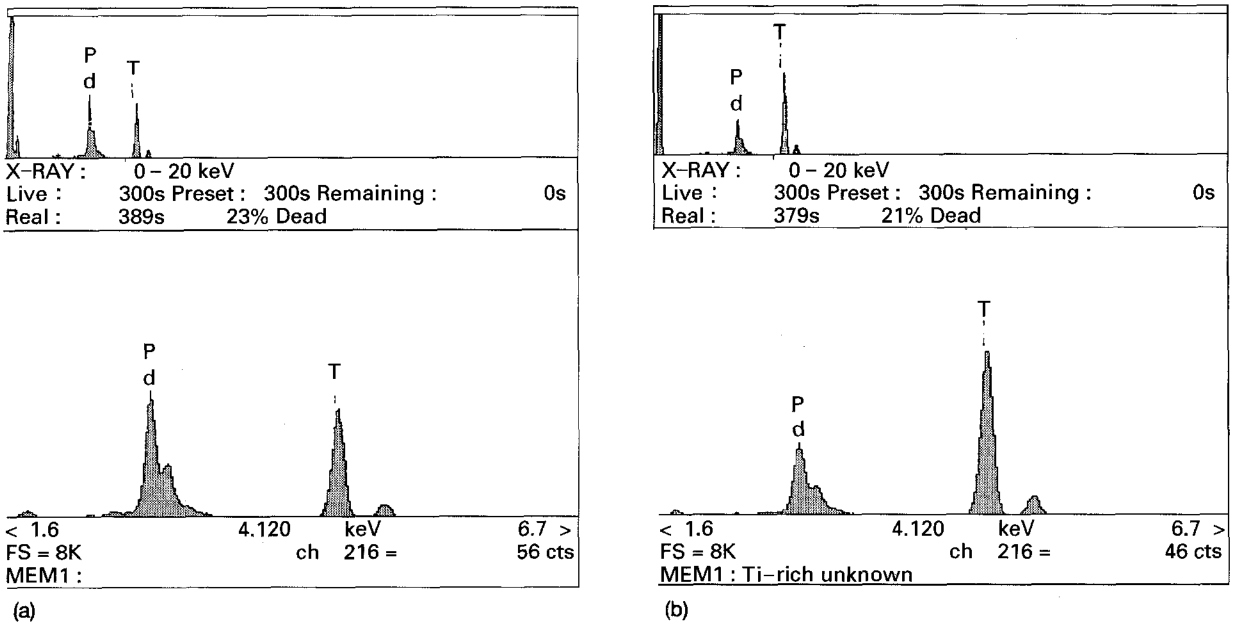

Figure 5 STEM/EDS spectra for (a) martensite matrix and (b) a second-phase particle of Ti$_{50}$Pd$_{50}$ alloy.

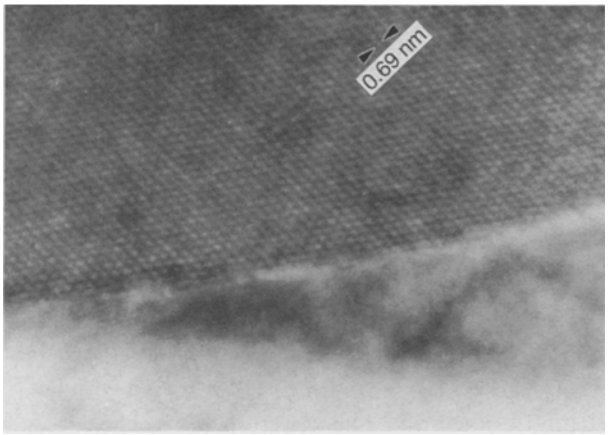

Figure 6 [$1\bar{1}01$] high-resolution electron micrograph of the second-phase particle showing the lattice image.

shown a Ti–Pd phase diagram with various intermetallic phases, for example, Ti_4Pd_3, Ti_3Pd_5, Ti_4Pd, etc. [15]. It is noted that none of the phases in their diagram corresponds to the present new phase.

4. Conclusions

A new phase in an equiatomic TiPd alloy has been identified using analytical electron microscopy. The phase is found as ellipsoidal particles along the grain boundaries of the martensitic matrix. The crystal structure of this phase has been identified as trigonal, with lattice parameters of $a = 0.83$ nm and $c = 2.62$ nm, and the point group is determined to be $\bar{3}\,m$. The chemical composition is shown to be 68–73 at % Ti ($\simeq$ 48–54 wt % Ti).

Acknowledgement

The authors acknowledge the financial support of this research by the National Science Council (NSC), Taiwan under the Grant NSC 80-0405-E002-08.

References

1. K. OTSUKA and K. SHIMIZU, *Int. Met. Rev.* **31** (1986) 93.
2. S. MIYAZAKI and K. OTSUKA, *ISI J. Int.* **29** (1989) 353.
3. T. TADAKI, K. OTSUKA and K. SHIMIZU, *Ann. Rev. Mater. Sci.* **18** (1989) 1.
4. V. N. KHACHIN, N. M. MATVEEVA, V. P. SIVOKHA, D. B. CHERNOV and YU. K. KOVNERISTYI, translated from *Dokl. Akad. Naud. SSSR.* **257** (1981) 167.
5. N. M. MATVEEVA, YU. K. KOVNERISTYI, A. S. SZVINOV, V. P. SIVKHA, and V. N. KHACHIN, *J.Phys.* **43** (1982) C4-249.
6. V. P. SIVOKHA, A. S. SAVVINOV, V. P. VORNIN and V. N. KHACHIN, *Phys. Met. Metal.* **56** (1983) 112.
7. A. L. LOTOKOV, V. N. GRISHKOV and V. V. FADIN, *Phys. Status Solidi* **70a** (1982) 513.
8. Y. C. LO, S. K. WU and C. M. WAYMAN, *Scripta Metall. Mater.* **24** (1990) 1571.
9. H. C. DONKERSLOOT and J. H. N. VAN VUCHT, *J. Less Common Metal* **20** (1970) 83.
10. J. L. MURRAY, in "ASM Handbook, Vol. 3, Alloy Phase Diagrams", (ASM International, Ohio, USA, 1992) pp. 2–341.
11. M. H. LORETTO, in "Electron Beam Analysis of Materials" (Chapman and Hall, London, 1984) Ch. 4.
12. B. F. BUXTON, J. A. EADES, J. W. STEEDS and G. M. RACKHAM, *Phil. Trans. R. Soc. A* **281** (1976) 171.
13. T. HAHN (ed.), "International Tables for Crystallography", Vol. 4. (The International Union of Crystallography, Derdrecht, Holland, 1983) Vol. 4.
14. G. CLIFF and G. W. LORIMER, *J. Microscopy* **103** (1975) 203.
15. H. C. YI, J. J. MOORE and A. PETRIC, *Metall. Trans. A* **23** (1992) 59.

Received 21 September 1992
and accepted 8 June 1993